November 30, 2000
VERSION 3.1

Algorithm Theoretical Basis Document (ATBD) for the AMSR-E Snow Water Equivalent Algorithm

Alfred T.C. Chang/Code 974
NASA/GSFC
Albert Rango/Hydrology Laboratory
USDA/ARS

With contributions from:

Norman Grody/Office of Research
NOAA/NESDIS

Alan Basist/NCDC
NOAA/NESDIS

Tom Carroll/NOHRSC
NOAA/NWS

Edward Josberger
Washington District
USDI/USGS

Leung Tsang
University of Washington

Barry Goodison and Anne Walker
AES/Canada

Richard Armstrong
University of Colorado

Richard Kelly
Birkbeck College,
University of London

Table of Contents

.

1.0 Introduction

The purpose of the AMSR-E snow mapping algorithm is to generate a global snow storage index map (SWEMAP) as a standard product from AMSR-E data. SWEMAP will be generated on a daily basis from the resampled swath data (Level-2A data) and output onto an equal area grid (Level-3 product). Pentad (five days) and monthly snow storage products will also be produced as a Level-3 product. These snow products will then be archived at the National Snow and Ice Data Center (NSIDC) Distributed Active Archive Center (DAAC) at the University of Colorado in Boulder. Snow depth maps will be considered as special products to be available after the launch and will not be discussed in detail in this document.

SWEMAP is currently structured to identify snow by its unique microwave brightness temperature properties. Snow crystals are effective scatterers of microwave radiation. When microwave radiation passes through the snowpack, its intensity is modified by the snow crystals. In general, the larger the snow water equivalent (SWE) value, the more snow crystals are available to scatter microwave energy away from the sensor. Snow detection is based on a series of criterion tests and decision rules that identifies snow. A physical retrieval algorithm will then be used to infer the SWE values. However, due to the complexity of snow water equivalent retrieval, rigorous validations are needed to ensure the quality of these retrieved SWE values.

In this revised Algorithm Theoretical Basis Document (ATBD), the methodology that is currently planned for use in mapping snow storage with AMSR-E data is discussed. The basic techniques used are thresholding, criteria tests, brightness temperature gradients, neural network and decision rules. A time and location dependent algorithm is now being developed for better derivation of snow water equivalent. This algorithm is currently tested and evaluated using the DMSP SSM/I data. Plans for algorithm validation and error analysis are also described.

The development of algorithms to map snow water equivalent is an evolutionary process. The precise algorithms may change as input ancillary data and our knowledge of the snowpack physics improves. The algorithms are likely to change after the snow profile ensemble evolves, and again after AMSR-E is launched. At that time, the full capabilities of the AMSR-E sensor can be realized and utilized to optimize the derivation of snow water equivalent values.

2.0 Overview and Background Information

2.1 Experimental Objective

The objective of this effort is to develop and implement algorithms that will map snow storage, and provide statistics of the global snow storage information over one day, 5

days and one month. The snow storage products will consist of daily estimates (Level-3 products) and combine daily estimates to create a map of pentad and monthly global snow storage (Level-3 product). Both Level-3 products will be gridded in an equal area projection in azimuthal format for the Northern and Southern Hemispheres.

The snow products may be used for monitoring the variability and measuring the changes or trends in hemispheric and global snow storage. Global snow storage is a key indicator of regional or global climate change, thus it is vital to have an accurate, consistent and validated data set to study the snow variability. It has been shown that global climate models do not simulate the present Arctic climate very well (Bromwich et al., 1994); improved measurements of global snow storage and other cryospheric elements are necessary to improve the modeling scenarios.

The AMSR-E snow maps will extend and augment the valuable record of Nimbus-7 Scanning Multi-channel Microwave Radiometer (SMMR) snow maps for the period of November 1978 to August 1987 (Chang et. al., 1987) and currently Special Sensor Microwave Imager (SSM/I). The ultimate goal is to combine SMMR, SSM/I and AMSR-E snow maps to create a long time series of snow product. The higher spatial resolution of the AMSR-E, relative to the SMMR and SSM/I, is likely to permit an improved ability to map snow storage in forest covered areas and mountainous regions, which presented problems when using SMMR or SSM/I data.

AMSR-E derived snow maps will be available as inputs to regional-scale hydrological models and general circulation models (GCMs). This will lead to better simulations of large-scale runoff. Also, since the global energy balance is strongly influenced by snow storage because of its high reflectivity, insulation properties, and the large amount of latent heat consumed during melting, the ability to derive accurate snow storage measurements will lead to better estimates of global energy distribution. Accuracy requirements for these applications are in the 10 to 20% range.

The AMSR-E snow water equivalent map (SWEMAP) product will complement the suite of snow products planned for the MODIS sensors. For example, snow surface albedo, snow surface temperature and snow-cover extent products will also be available for research. A microwave sensor which is not strongly affected by the cloud, can provide additional information of the snowpack when it is cloud obscured .

2.2 Historical Perspective

Development of the microwave snow depth and snow water equivalent algorithm is based on experiences gained using the Nimbus-7 SMMR and DMSP SSM/I data. SMMR data have been used to map global snow depth with some success (Chang et al., 1987). For the last several years, the Canadian Atmospheric Environment Service has used the near real time SSM/I data to derive snow water equivalent values over the Canadian prairies for

hydrological and climatological applications (Goodison and Walker, 1993). The National Operational Hydrologic Remote Sensing Center (NOHRSC) of the National Weather Service (NWS) is studying the inclusion of SSM/I data, in addition to airborne gamma, and meteorological station data to produce snow equivalent values for North America during the winter season (Carroll, 1997).

2.2.1 Remote Sensing of Snow Extent, Depth and Water Equivalent

Satellite sensors have been deployed successfully to study snow extent, depth and water equivalent. NOAA has used data from the Scanning Radiometer (SR), Very High Resolution Radiometer (VHRR) and Advanced Very High Resolution Radiometer (AVHRR) sensors since 1966 to produce snow extent maps using the visible and near-IR sensors (Matson et al., 1986; Matson, 1991). Passive-microwave sensors on-board the Nimbus 5, 6, and 7 satellites and the Defense Meteorological Satellite Program (DMSP) satellites have been used successfully for measuring snow extent at a 25- to 30-km resolution through cloud cover and darkness since the 1970s. Passive-microwave sensors more importantly could provide information on snow depth (Foster et al., 1984). With the launch of the Terra satellite, MODIS data snow cover estimates will greatly improveSnow cover mapping capabilities.

The early passive microwave snow studies took place at the end of the 1960's when ground based microwave radiometers showed the potential of inferring snow parameters. Microwave brightness temperature measured by space-borne sensors originates from (1) radiation from the underlying surface, (2) the snowpack, and (3) the atmosphere. The atmospheric contribution usually is small and can be neglected over snow covered areas. Under this condition, microwave measurements can be used to extract snowpack parameters. Snow crystals are effective scatterers of microwave radiation. The deeper the snowpack, the more snow crystals there are available to scatter microwave energy away from the sensor. Hence, microwave brightness temperatures are generally lower for deep snowpacks (more scatterers) than they are for shallow snowpacks (fewer scatterers, Matzler, 1987; Foster et al., 1991). Based on this fact, snow water equivalent retrieval algorithms were developed (Kunzi et al., 1982; Chang et al., 1982; Hallikainen and Jolma, 1986; Goodison et al., 1990; Rott et al., 1991).

From November 1978 to August 1987, SMMR on board the Nimbus-7 satellite, acquired passive microwave data (Chang et al., 1987). Using a single algorithm based on the theoretical radiative transfer calculations, monthly global snow depth maps were generated. This data set was archived by NASA's Pilot Land Data System (PLDS, 1990) and later by the National Snow and Ice Data Center (NSIDC).

The quality of the SMMR-derived snow depth data set has been carefully studied and evaluated by many investigators (e.g. Barry and Schweiger, 1988; Robinson et al., 1993; Tait and Armstrong, 1996). It was found that the SMMR snow data set performed well

in the prairie regions compared with NOAA snow maps, but performed poorly in some parts of the boreal forest and high latitude tundra regions. Comparisons of derived snow storage with climatological data and with outputs from several GCMs revealed that the SMMR data probably underestimates the global snow storage by about 50% during the winter months (Foster, 1995). Based on these investigations, we were able to identify areas where the SMMR algorithm needed improvement.

2.2.2 Problems Associated with Snow Cover Retrieval Algorithms

Two problems in the radiative transfer calculations (Chang et al., 1991) are the assumptions related to the snow grains, namely (1) spherical shape, and (2) independent scatterer. These assumptions have mostly been resolved using a much improved radiative transfer model for a densely packed snow. In a densely packed snow, the scattering particles' position affect the scattering physics and invalidate the independent scattering assumption. To account for the correlation between particles, a quasicrystalline approximation (Tsang and Kong, 1980) and a quasicrystalline approximation with coherent potential (Tsang and Kong, 1980) have been used. The dense media radiative transfer calculations (Tsang and Kong, 1992) are currently being used to address the independent scatterer issue. Snow crystals tend to cluster in a snowpack after extended metamorphosis. By applying a sticky particle distribution function (Ding et al., 1994, Zurk et al., 1995) it is possible to account for the clustering of non-spherical snow grains in snowpacks. Tsang et al. (2000) was successful in matching the SSM/I brightness temperature with values derived from this model.

Foster et al. (1999) compared the calculated cross-section of different shapes of crystals using a discrete dipole scattering model (Draine and Flatau, 1994). The model results demonstrate that the shape of the snow crystal (spheroids, cylinder, cubes, ellipsoids, tetrahedrons and hexahedrons used) makes an insignificant contribution to the electromagnetic response from snow. This finding considerably relaxes the limitation of the spherical crystal assumption.

Because crystal size and shape is evolving continuously after deposition on the Earth's surface, it is necessary to take into account the crystal size growth with time (Armstrong et al., 1993). Snow crystals grow largely due to the temperature gradients within the snowpack. There are empirical and numerical models that have been developed to predict the growth of the snow crystal (e.g. Navarre, 1974; Marbouty, 1980). Jordan (1991) included the granular growth rate in her one dimensional temperature snow cover model which was tested over Greenland with some success (Nolin and Stroeve, 1996). Brun et al. (1992) have successfully modeled the grain growth for operational avalanche forecasting. After extensive tests of the grain growth formula, it is rather difficult to select one that is best suited for our purpose. Recently, Josberger et al. (1995) reported that the first snow of a new season has a dominated influence on the snow crystal growth for that year. This could complicate the snow retrieval algorithm because the algorithm is

very sensitive to the first estimate of snowpack crystal structure and information on initial crystal structure is not collected routinely by operational snow monitoring organisations.

Forests present perhaps the biggest challenge to develop a robust microwave SWE retrieval algorithm. Kruopis et al. (1998), using 6.8, 10.7 and 18.7 GHz data, successfully inferred quantitatively the forest stem volume. Thus, with the lower frequency data, AMSR-E data may be able to provide further forest volume information. At present, a forest cover distribution map is used to correct for the effect on the microwave signal. Robinson and Kukla's (1985) maximum albedo map (one degree by one degree spatial resolution) is used for this purpose. This is because there is an inverse relationship between the forest density and surface albedo.

To assist with the forest fraction issue, a 1 km land use classification map has been made available by the MODIS land group. The data are a useful first attempt to assimilate these data although a comparison study showed that land use classification map may not represent the forest density. Therefore, we are still searching for a forest density map with right spatial resolution to improve the quality of the snow retrieval.

Varying meteorological conditions produce different regional snowpack characteristics. Layer and grain distributions are time-dependent and change with the weather. Recently a new classification system for seasonal snow covers was reported by Sturm et al. (1995) which divides seasonal snow covers into six classes (tundra, taiga, alpine, maritime, prairie, and ephemeral). Each class is defined by a unique ensemble of snowpack textural and stratigraphic characteristics: snow stratigraphy, thickness, density, crystal morphology, and grain characteristics. Groups of different snow profiles will be adopted for each snowpack class in the retrieval algorithm.

Liquid precipitation can affect the microwave signatures over land. Spencer et al. (1989) reported the successful detection of heavy rainfall over land in many cases. Grody (1991) reported that it is necessary to remove the rain signal to discriminate snow cover. Thus, when rain is detected, snow parameters may not be retrieved and it will be flagged as 'rain'. Grody's multi-frequency procedure to filter the rain cases is adopted to remove the pixel that is affected by the rain signal.

When the snowpack is wet, microwave responses change drastically. The presence of liquid water within the snowpack alters the microwave emission characteristics such that internal absorption increases significantly. Walker and Goodison (1993) reported a method to detect wet snow cover using passive microwave data for the Canadian Prairies. They showed that an abrupt brightness temperature change occurs when the air temperature is closer to 273 K this effect can provide an opportunity to delineate the region where the snowpack is melting. In such cases, no SWE estimate will be produced and is the cell will be flagged as 'wet snow'.

Since the AMSR-E footprint for 19 GHz is about 24 x 24 km^2 , a mixture of different features within a footprint can be expected. To improve the accuracy of estimated SWE, surface composition information and the time history of the snowpack are needed. A fixed earth grid is needed for an easy accumulation of the ancillary information. We will adopt the NSIDC Equal Area SSM/I Earth (EASE) grid system to store the ancillary snowpack and surface information. This grid system was first developed by the SSM/I Land Products Working Team (SPWT) and later adopted by the NOAA/NASA SSM/I Pathfinder Team to produce the pathfinder data sets. Under the EASE grid system, each grid is pre-defined. We will create raster files of snow classification, vegetation cover, grain size information as well as the land cover classes for each EASE grid pixel. Percentages of different land cover classes, such as conifer trees, deciduous trees, bare soil, grasslands, impervious areas, etc. will also be assigned. Currently EASE grid has two grid size, 25 km and 12.5 km respectively. For AMSR-E snow algorithm, a 25 km grid will be used. A simple gridding routine has been developed to project the Level 2A data onto the EASE grid.

Estimating snow storage in the mountainous region is a challenging task. This is because the complex topography together with the protruding exposed rocks within a microwave footprint make it difficult to extract the snow signature. The AMSR-E 19 and 37 GHz footprint will not be able to resolve the complicated terrain effects. Besides, different viewing direction of the mountain by the ascending and descending orbits further complicates the problem. We will not pursue to include elevation correction in the pre-launch version. Therefore, pixels in mountainous terrain may not give accurate SWE estimates and will be flagged based on the roughness factor derived from the digital terrain data.

2.2.3 Remote Sensing of Snow on the Greenland and Antarctica Ice Sheets

Most of the fresh water on Earth is stored in Greenland and Antarctica ice sheets. The most critical aspect of these ice sheets is their potential in affecting global sea level. These ice sheets also influence the global climate system through their high albedo and elevated topography.

Snow continuously accumulates on most of the Greenland and Antarctica ice sheets. A long and detailed record of past climatic and atmospheric conditions exists in the annual layers of snow deposited in regions where surface melting seldom occurs. Areas in the southern part of the Greenland experience periods of surface melting each summer. If climate warming scenarios are proven, the melt areas and the rates of melting probably will increase. Microwave signals are most sensitive to the wetness in snowpack and may be able to delineate the melting area accurately.

The characteristics of the accumulated snow in Antarctica and Greenland are different from the continental seasonal snowpacks. Due to continuous densification of accumulated snow and crystal bonding, brightness temperatures emerging from an ice sheet are different from the seasonal snowpack (Abdalati, 1996). Therefore, a different snow retrieval algorithm will be needed to account for the layers of snow over the ice sheets. Layered models have been proposed (West et al., 1996; Grody and Basist, 1997) to explain the low brightness temperature observed over the ice sheets. Wisemann and Matzler (1999) developed a radiative transfer model for layered snow. However, at this moment, no applicable passive microwave algorithm has been developed to infer the information of the snow layer on top of the ice sheets with any accuracy. This issue will be defered until after the launch of the Aqua satellite.

Over ice sheets the total snow water equivalent is not very well defined.. Instead, annual snow accumulation rate, which is directly related to ice sheet dynamics, is important to global change research. Microwave emission from Antarctic firn has been shown to be correlated with the annual mean temperatures and snow accumulation rates (Zwally, 1977; Fily and Benoist, 1991). The prevailing view of the ice sheet response to climatic change is that a global warming will enhance melting of the Greenland ice sheet, and enhance snowfall on the Antarctic ice sheet with little net effect on sea-level. However, any changes of snow accumulation rate in Greenland and Antarctica may be a useful indicator of global climate change. We will investigate the possibility of using lower frequency (6.9 and 10.7 GHz) which is more sensitive to snow layering temperature properties, to infer the snow accumulation rate over the ice sheets after the AMSR-E data become available.

2.3 Instrument Characteristics

The EOS Aqua AMSR-E is a twelve channel, six frequency total power passive microwave radiometer system. It measures brightness temperatures at 6.925, 10.65, 18.7, 23.8, 36.5, and 89.0 GHz. Vertically and horizontally polarized measurements are taken at all channels. This sensor is different from the AMSR on ADEOS-II; the EOS Aqua AMSR sensor is designed as AMSR-E.

The instrument, modified from the design used for the ADEOS-II AMSR, consists of an offset parabolic reflector 1.6 meters in diameter, fed by an array of six feedhorns. The reflector and feedhorn arrays are mounted on a tub, which contains the radiometers, digital data subsystem, mechanical scanning subsystem, and power subsystem. The reflector/feed horn/drum assembly is rotated about the axis of the drum by a coaxially mounted bearing and power transfer assembly. All data, commands, timing and telemetry signals, and power pass through the assembly on slip ring connectors to the rotating assembly.

A cold load reflector and a warm load are mounted on the transfer assembly shaft and do not rotate with the drum assembly. They are positioned off axis such that they pass between the feedhorn array and the parabolic reflector, occulting it once each scan. The cold load reflector reflects cold sky radiation into the feedhorn array thus serving, along with the warm load, as calibration reference for the AMSR. Calibration of the radiometers is essential for collection of accurate data. Corrections for spillover and antenna pattern effects are incorporated in the data processing algorithms.

The AMSR rotates continuously about an axis, parallel to the local spacecraft vertical, at 40 rpm. At an altitude of 705 km, it measures the upwelling scene brightness temperatures over an angular sector of +/- 70 degrees about the sub-satellite track, resulting in a swath width of 1500 km.

During a period of 1.5 seconds the spacecraft sub-satellite point travels 10 km. Even though the instantaneous field-of-view for each channel is different, active scene measurements are recorded at equal intervals of 10 km (5 km for the 89 GHz channels) along the scan. The half cone angle at which the reflector is fixed is 46.6 degrees which results in an Earth incidence angle of 53.9 degrees.

Aqua AMSR-E Performance characteristics

Center Freq (GHz)	6.9	10.7	18.7	23.8	36.5	89.0
Band Width (MHz)	350	100	200	400	1000	3000
Sensitivity (K)	0.3	0.6	0.6	0.6	0.6	1.1
IFOV (km x km)	76 x 44	49 x 28	28 x 16	31 x 18	14 x 8	6 x 4
Sampling Rate (km x km)	10 x 10	10 x 10	10 x 10	10 x 10	10 x 10	5 x 5
Integration Time (msec)	2.6	2.6	2.6	2.6	2.6	1.3
Main Beam Efficiency (%)	95.3	95.0	96.4	96.4	95.3	96.0
Beam Width (deg)	2.2	1.4	0.8	0.9	0.4	0.18

2.3.1 Radiometer Calibration

The radiometer calibration accuracy budget, exclusive of antenna pattern correction effects, is composed of three major contributors: warm load reference error, cold load reference error, radiometer electronics nonlinearities and errors. Each error component is discussed in the remaining paragraphs of this section. Accounting for all errors, the total sensor bias error is 0.66 K at 100 K and changes with temperature to 0.68 K at 250 K.

2.3.1.1 Warm Load Reference Error

The major part of this error comes from the following four components:

a) the accuracy of the platinum resistance thermistors (PRTs), measured by the manufacturer, on of the order of 0.1 K;
b) the temperature gradient over the load area (the SSM/I load temperature varies as high as +/- 0.4 K);
c) load - feedhorn coupling errors due to the design of the system, and
d) reflections out of the feedhorn due to receiver electronics. An estimate of the warm load reference error, when using the aforementioned components, is 0.5 K.

2.3.1.2 Cold Load (cold sky reflector) Reference Error

The error in the cold reference measurement is mainly produced by the error in coupling between the cold sky reflector and the feedhorn. This is estimated to be 0.5 K. Other factors affecting the cold reference error are the reflections out of the feedhorn due to receiver electronics and the resistive losses of the cold sky reflector itself. An estimate of this error can be as high as 0.62 K.

2.3.1.3 Radiometer Electronics Nonlinearities and Errors

The main factor that drives the electronics nonlinearity is the imperfect operation of the square law detector. This nonlinearity results in an error that can be estimated during the thermal vacuum calibration testing. (On SSM/I this error was 0.4 K.) A source of error due to the receiver electronics is the gain drift due to the temperature variation over one orbit. This error depends on the design of the receiver and overall design of the sensor. This drift can be as much as 0.24 K for a temperature variation of less than 10^{o} C over one orbit.

3.0 Algorithm Descriptions

3.1 Theoretical Descriptions

3.1.1 General Description of the Snow Algorithm

The intensity of microwave radiation emitted from a snowpack depends on the physical temperature, grain size, density and the underlying surface conditions of the snowpack. By knowing these parameters, the radiation emerging from a snowpack can be derived by radiative transfer computation. The scattering properties of densely packed spherical and non-spherical particles have been calculated (Tsang, 1992). The calculations are based on analytic multiple scattering theory and numerical solutions of Maxwell's equations. The model takes into account the individual particle scattering characteristics as well as the collective coherent scattering effects as dictated by the packing and the relative positions. While the vertical structure of the snowpack is extremely critical in determining upwelling microwave radiances, it cannot be easily characterized in terms of a single unknown variable. An ensemble of snowpack profiles have been selected to represent different snow conditions for different snow classes. Brightness temperatures were calculated

using the dense media radiative transfer equation. At present, only 19 GHz V and H and 37 GHz V and H polarization have been calculated. We will continue to extend the radiative transfer calculations to other AMSR-E frequencies.

There are many factors that can affect the microwave brightness temperature emerging from a snowpack. For example, the freeze/thaw states of the underlying soil, crystal size profile, temperature profile, density profile, and the layering structure can alter the microwave signature. This algorithm utilizes an inversion scheme, which attempts to overcome some of these problems by simultaneously retrieving the parameters of the snowpack. A modeled multi-channel brightness temperature database is calculated on these snow parameters.

Once a database of snow profiles and associated brightness temperatures is established, a multi-layer perceptron (MLP) type artificial neural network (Chang and Tsang, 1992) is used. The MLP type of neural network consists of one input layer, one or more hidden layers and one output layer. Each layer employs several neurons and each neuron in the same layer is connected to the neurons in the adjacent layer with different weights (Figure 1). The activity at an input neuron represents the value of some input signal. Signals pass from the input layer, through the hidden layers to the output layer. Except for neurons of the input layer, each neuron receives a signal, which is a linearly weighted sum of all the outputs from the neurons of the formal layer. The backpropagation learning algorithm is employed for training the neural network. In short, this algorithm uses the gradient descent algorithm to obtain the best estimates of the interconnected weights, and to force the output network to be as close to the desired values as possible for the given input training sets. Since the development of a database is very complex, with many adjustable parameters, simple regressions are currently used for at launch SWE estimates.

3.1.2 SWEMAP

Figure 2 is a flow chart of the outline of the SWEMAP processes. A granule (one half of an orbit) of data will be the unit for AMSR-E processing. The first step in producing the granule SWEMAP is to obtain the corresponding attributes of the grid. This includes (1) snow classes, (2) fractional forest cover, (3) land use classes, (4) elevation, (5) probability of snow, (6) SWE history and (7) land mask to discriminate ocean, land and ice sheets. After collecting the ancillary data from the database a sequence of tests will be conducted to select a group of snow conditions that will best match the AMSR-E observations.

After ingesting the AMSR-E Level-2A data, these data will be projected onto an EASE grid for processing. A series of tests will be performed on the AMSR-E data. The first test is on the probability of snow. For those grids located in a region where the probability of snow is zero, no snow is assumed. The snow frequency maps were derived from the ten years of weekly snow and ice charts of the Northern and Southern Hemisphere (Dewey and Heim, 1981 and 1983). This test is necessary to eliminate the

possibility of misclassifying desert and other scattering surface (which scatters microwave energy) as the snow cover.

Next, for each grid cell, a rough surface temperature (either snow covered or snow free) will be estimated using the method described by Pulliainen et al. (1997). These estimated temperatures will be used to determine whether the presence of snow cover is possible for this grid cell; a threshold (~273K) is used to to this effect. Previously, empirical brightness temperature thresholds ($T_{B37V} > 250K$, and $T_{B37H} > 240K$) were used. If the presence of snow is detected in the grid cell, the snow algorithm is applied to the grid cell. When rain or wet snow is detected, no accurate SWE estimates can be produced. After it is decided that dry snow is possible, fraction of forest cover and other types of land covers will be used to narrow down the selections in the data ensemble from the neural network SWE estimator.

Before applying the snow algorithm, tests for unfrozen soil, shallow snow and powder snow will be conducted. Different brightness temperature snow water equivalent relationships will be applied accordingly. The 89 GHz channel signal over snow is the key frequency in determining the shallow snow and power snow information. At the time of the compilation of this report, some of these tests are still being developed and evaluated. By constraining the brightness temperature ensemble, improved snowpack parameter estimates are expected.

3.1.2.1 Detailed description of SWEMAP algorithm

The output from SWEMAP is a three dimensional array in a binary raster format (1 byte per pixel). Assuming the array is called 'out', its dimensions are arranged as out[flag,nrows,ncols] where 'flag' is an integer from 0 to 2 where 0 is flag number, 1 is SWEMAP (mm) and 2 is SDMAP (cm), nrows is the number of lines (rows) and ncols is the number of pixels (columns). The methodology generally described in 3.1.2 above translates into the following precise method.

Daily SWEMAP/SDMAP generation			
Operation	**Data**	**Source**	**Flag**
I. ***Ingest ancillary spatial data files into 25 km EASE-grid arrays.***	snow pack climatology fractional forest cover land use classes elevation snow probability dynamic SWE data dynamic frozen ground data	Sturm et al., 1995 Robinson & Kukla, 1985 MODIS land group EDC/USGS Dewey and Heim, 1981 & 1983 from previous day from previous day	
II. ***Ingest ancillary time dependent data files into temporal arrays.***	grain size	Josberger and Mognard (2000) & GSFC data base.	
III. ***Ingest AMSR Level 2A and navigate data to EASE-grid.***	MSFC (Huntsville) Level 2A desription	(See http://www.ghcc.msfc.nasa.gov/AMSR/html/tlscf.html)	

IVa. Determine a pixel snow impossible.	If snow impossible, flag no snow and continue to next pixel.		252,253, 254,255
IVb. Determine a pixel snow possible	If snow possible, screen for different surfaces. (See V)		
V. Screenings	Approximate surface temperature: AMSR Tbs No land snow: (flag and next pixel) Precipitation: (flag and next pixel) Frozen Ground: (flag and next pixel) Wet snow determination (flag and next pixel) Dry snow determination (see VI and VII))	Pulliainen et al. (1997), GSFC development. Grody and Basist (1996) Grody and Basist, (1996) Grody and Basis, (1996). Update dynamic frozen ground file. Walker and Goodison (1993), Sun et al. (1996), Basist et al. (1997)	 252 250, 251 252 249 1-7
VI. SWE estimation	Mountains Forests Other Update dynamic SWE data file	GSFC Development Chang et al. (1997) Chang et al. (1997)	
VII. SD estimation	SWEMAP	GSFC development	

Pentad SWEMAP generation is maximum SWEMAP in 5-day period

Monthly SWEMAP is average SWEMAP for each month

3.1.3 Calculation and Testing Technique

The following tests are performed on the gridded brightness temperature before the snow determination. Criteria of these tests are tabulated in Table 1.

3.1.3.1 Surface Temperature

Surface temperature inferred from satellite radiometer measurements has been attempted using the infrared bands (Davis and Tarpley, 1983). When the cloud is not completely opaque infrared data can be able to correct for the atmospheric absorption due to clouds and water vapor and derives the surface temperature. Surface temperature will be a standard MODIS product on a climate model grid (1/4º by 1/4º resolution). Difficulties in using the MODIS derived surface temperature are (1) frequent cloud cover and (2) timely data availability. Since EOS Terra MODIS data will be in orbit two years ahead of AMSR-E, we will evaluate the quality of its derived surface temperature. If MODIS surface temperatures are available and adequate for AMSR-E processes, we will utilize the MODIS temperature data.

Recently, microwave measurements have been used to infer the land surface temperature. At the microwave frequencies the effects of atmospheric absorption can often be

neglected, however, one must account for the larger variations of the surface emissivity. Pulliainen et al. (1997) reported surface temperature retrieved in the boreal forest zone using SSM/I data. The physical temperature at the surface can be retrieved with an accuracy of 1.2 to 2.5^{o}C. Regression relationships for temperatures over alpine, taiga, tundra and prairie regions were derived for selected stations. Basist et al. (1997) reported that surface temperature derived during the 1996 blizzard condition had a standard error of 2^{o} C. They also corrected for the surface emissivity change due to soil moisture. We implemented the Basist et al. (1997) surface temperature algorithm to screen areas where snow is possible (see also Williams et al. 2000). Due to the accuracy of surface temperature derived from microwave data, the temperature threshold for wet snow and no snow will be lower by 2.5^{o} C.

3.1.3.2 Precipitation

Over land, rain detection is problemmatic when using AMSR-E microwave emission signals. The high frequency band of the microwave spectrum (> 85 GHz) can detect ice particles aloft in precipitation and snow on ground (Grody and Basist, 1997). The density and size of rain particles are often larger than snow crystals on the ground surface. Based on these principles, precipitation can be identified. We use the rules developed by Grody and Basist (1996) to screen the grid cells for rain.

3.1.3.3 Wet Snow

The wet snow signature is distinctly different from the dry snow signature. When the snow is wet, 19 and 37 GHz brightnes temperatures are not able to determine the SWE or depth accurately. With the additional 6 and 10 GHz, AMSR-E might be able to provide the wet snowpack information. Walker and Goodison (1993) reported a wet snow discrimination technique based on the 37 GHz polarization differences. Sun et al. (1996) used a neural network to determine snow wetness in vegetated terrain. Both techniques were developed and calibrated for specific regions and require tuning when applied to different regions. We will work with both teams to improve the algorithm's wet snow detection capabilities. A simple rule that can also be followed is that when there is snow detected in the previous day and wet snow is detected in the following day, a wet snow condition is assured for the intervening days.

3.1.3.4 Fractional Forest Cover

Robinson and Kukla's maximum snow albedo map is currently used as the proxy for fractional forest cover. The maximum albedo value in the map is 0.8, which represents no forest. The minimum albedo value is 0.2, which represents 100 percent forest cover. Fractional forest cover is linearly interpolated between these two values. An EASE grid version of this data set has been prepared and archived by NSIDC.

3.1.4 Daily SWEMAP

The daily SWEMAP will be the composite of granules of SWE data within one day. Derived snow parameters from multiple passes over the same grid cell will be screened for consistency based on statistical tests. When more than one SWE estimate falls in a grid cell, the maximum snow storage will be recorded.

3.1.5 Pentad SWEMAP

The swath width for the AMSR-E is approximately 1600 km. There will be gaps between the AMSR-E adjacent orbital swath data, thus gaps in inferred daily SWEMAP. For the research community there is a need for a global snow data set. After discussions with NSIDC personnel, it is found that the pentad snow product is the most commonly used product by climate and cryospheric researchers.

The pentad SWEMAP will consist of the composite of the daily SWE data. Derived snow parameters from daily product over the same grid cell will be screened for consistency based on statistical tests and maximum snow storage will be produced. There are 73 pentads in a year and for leap years the pentad including February 28 will have an extra day.

3.1.6 Monthly SWEMAP

The monthly SWEMAP will be generated by composite of the daily SWE data. Derived snow parameters from daily product over the same grid cell will be screened for consistency based on statistical tests. Mean snow storage for the month will be produced.

3.1.7 SDMAP

When calculating the brightness temperature ensemble, snow depth is one of the input parameters. Relationships between snow depth and microwave brightness temperature are built in to the data ensemble. The neural network can also be used to infer the snow depth from observed brightness temperatures. At this moment we have not thoroughly investigated the quality of the derived snow depth product and so it will be considered as a special product after launch.

3.2 Error Estimates

3.2.1 Variance or Uncertainty Estimates

The goal of the AMSR-E snow algorithm is to develop an algorithm that is as physically based as possible and produces SWE within well defined error bounds. Scattering of

upwelling microwave radiation by the snow crystals is used to infer the total snow storage. Physically based algorithms have the advantage that their applicability to various snow conditions can be tested and verified by examining the physical assumptions made in the models. However, there are many uncertainties in the model parameterisation that could affect the successful mapping of snow water equivalent. Varying snow crystal sizes, snow detection in mountainous terrain, wet snow discrimination and mapping snow in densely-forested areas are some of the problems that will affect the errors in snow mapping using AMSR-E data. These factors can also be spatially heterogeneous and produce variable snow cover conditions within the AMSR-E footprint. Therefore, the variance of estimated SWE within a footprint can be great.

3.2.2 Algorithm-Related Error Sources

Some sources of error in mapping snow storage using SWEMAP are shown below. Errors are expected to be caused by:

1) obscuration by dense liquid water clouds, rain, and dense forests;
2) inability to map the water equivalent of partially wet snow covers;
3) maximum pentad snow storage will not exactly represent the average pentad snow storage;
4) mapping snow in topographically-rough areas as if they were flat; and
5) inaccuracy in the atmospheric correction. This is due to the fact that retrieved cloud water content over land is not accurate, estimated average snow grain size will be different from the actual grain size (a problem related to the lack of available and timely meteorological data), and estimated surface temperatures being different from the actual surface temperatures.

Sensitivity of each error source will be evaluated and quantified before the launch of EOS Aqua satellite. One way this can be done is by simulation, varying each snow parameter incrementally and analyzing its effect on retrieval results.

3.2.3 Geographic and other Error Sources

Varying surface conditions, cloud climatology, and varying air temperature are potential sources of error in the SWEMAP. Extensive tests of the SWEMAP under different snow conditions will allow us to identify conditions under which SWEMAP generates reasonable results, and conditions under which SWEMAP generates questionable results. Before the launch of EOS Aqua satellite, SSM/I will be used to test the snow algorithms.

A large portion of the Earth's land surface is covered by dense forests. The boreal forest, the forest that stretches across the northern tier of North America and Eurasia, is a prime example. Snow accumulates to greater depths and melts later in the spring in the boreal forests than in adjacent tundra or prairie areas (Foster et al., 1991). The boreal forest

areas are always snow covered during the winter. Snow accumulated under the canopy typically exceeds that found in the open areas. However, even with a longer wavelength detector (5 cm), snow under a tree canopy is often not detected (Hall et. al., 1982; Foster et. al., 1991). It is expected that using the MODIS snow cover maps, detection of snow in these regions will be greatly improved.

3.3 Practical Considerations

The SWEMAP at-launch versions are not numerically intensive because of the low AMSR-E data rate. The numerical computation may increase as SWEMAP is changed to possibly include elevation and grain size models to generate more accurate snow-storage maps. The use of elevation data for snow mapping is currently being investigated.

EASE grid was developed at the NSIDC. We will work with NSIDC to obtain a copy of the software. If these gridding procedures are not included in the toolkit to support generation of output products, then gridding procedures unique to the algorithm products will be integrated into the snow algorithm software.

Reprocessing decisions are expected to be made after two years of snow data have been processed and analyzed. Enough experience should have been gained by that time to render a good assessment of the accuracy of the data sets generated by SWEMAP. Once AMSR is launched, more accurate coefficients of the snow water equivalent/brightness temperature relationship may be determined. If this provides results superior to the at-launch algorithm, then all the data will be reprocessed.

3.3.1 Programming/Procedural Considerations

Algorithms will be coded according to guidelines set forth by the EOSDIS. When practical, toolkits or utilities provided by the EOSDIS will be used and integrated into the algorithms. Procedures for coding and delivery of code, documents, etc. to EOSDIS will be followed to the extent possible. The algorithms will be coded in C and Fortran. Quality assessment products may be generated with output from the algorithms using commercially available software package(s), e.g. Interactive Data Language (IDL).

3.3.2 Calibration and Validation

The absolute calibration of each microwave sensor will be different. Therefore, we will have to perform a post launch adjustment of the coefficients for snow parameter retrieval, even though the snow algorithm is physically based. Snow water equivalent validation will be performed over selected test sites for different snow conditions (tundra, taiga, alpine, prairie, maritime and ephemeral) to assess the accuracy of the algorithm under

different snow conditions. Test sites associated with the snow classes will be selected where ground snow information is most readily available.

3.3.2.1 Point SWE vs. Areal SWE

Since the most readily available snow truth data is snow gauge data, point measurements are used as a validation source. However, comparisons of point measurements with satellite derived areal snow estimates for the last several years have been unsatisfactory. It is necessary, therefore, to re-design a workable strategy to determine how the validation of snow water equivalent values is to be achieved.

The number of samples required to accurately represent the SWE of a large field depends on the spatial variability of SWE within the large field and accuracy requirements. To be 95% confident that the true mean is within plus and minus L of the estimated mean, the number of sample n required is (Snedecor and Cochran, 1967)

$$n = (1.96\,\sigma/L)^2 \sim 4(\sigma/L)^2$$

For σ = 20 .mm and L = 10 mm, n = 16. In other words, we will need 16 gauges within a footprint that measure SWE variations of 20 mm accurate to +/- 10 mm. With four measurements the accuracy is +/- 20 mm. If there is only one measurement within the footprint, the expected accuracy is +/- 40 mm (twice the actual SWE variation within the footprint). In general, there is at most one gauge per grid cell the hence the accuracy is sub-optimum.

To test these constraints, gauge observations within a 2x2 EASE grid (approximately equals to a 50 x 50 km^2 grid) over the Northern Great Plains were compared with microwave estimates. With 2 to 3 measurements per grid cell the r^2 for snow depth and brightness temperature was approximately 0.6. When extended to a larger area in North Dakota (5x5 EASE grid) where there were 14 measurements within the grid box, an improved relationship between temporal and spatial dependence of snow depth and brightness temperature was obtained.

During February 1994, as a part of the BOREAS project, microwave radiometers (18, 37 and 92 GHz) were flown on a Twin Otter aircraft over the Canadian boreal forest region. Extensive snowfield measurements were acquired. A detail examination of these data found that it is possible to match the aircraft derived SWE and satellite derived SWE even in forested areas. Airborne microwave observation, thus, may be used to validate the satellite SWE estimates. For forested areas it is necessary to account for the grid cell percent of forest coverage for SWE estimates (Chang et al., 1996). During the experiment we found that the physical temperature of the tree was closely related to the surface temperature (Chang et al., 1997). Thus, for a improved estimates of SWE, surface temperatures are needed in conjunction with information about forest cover.

3.3.2.2 Statistical Approaches

Carroll et al. (1995) reported using a kriging model to incorporate snow gage data to areal SWE. Recently, results from a block kriging analysis of the snow water equivalent over the Ob River basin, Russia (Brubaker et al., 2000) showed that SSM/I derived SWE and the interpolated snow course SWE are comparable. A 2500 km north to south transect across the Urals was selected for the study. Data from snow courses in the Ob River basin were used to generate an optimally interpolated SWE map. When comparing the SWE estimates derived from SSM/I data and the interpolated station data, the differences were consistently well within two standard deviations of the kriged SWE. Due to the limited snow course observations in the Ob River basin, the standard deviation of interpolated SWE is large. However, this is the best SWE estimate for there are no other SWE available for comparison. We will use a similar statistical method to provide optimum estimates of snow storage from the areas where insufficient measurements are available from the ground-based network.

We are also collaborating with an ongoing NASA-funded project (NAG5-6636) at the University of Colorado (CU) National Snow and Ice Data Center (NSIDC), (Armstrong and Brodzik, 2000). This study involves the comparisons of six different passive microwave snow algorithms. These algorithms represent examples which include both mid- and high-frequency channels, vertical and horizontal polarizations and polarization difference approaches.

While SWE data are much less prevalent than snow depth data, there are numerous SWE data sets available for limited regions and over short periods of time. However, the CU/NSIDC project concentrates on those SWE data sets which are the most spatially and temporally comprehensive. The philosophy of this study is to focus on the robust nature of the larger validation data sets which is expected to provide a full range of snow/climate relationships rather than on smaller data sets which may only represent a "snapshot" in time and space.

In order to compare algorithms over a wide variety of snow cover and land surface types, the current phase of this study focuses on the data set "Former Soviet Union Hydrological Surveys" (FSUHS) which is archived at NSIDC (Haggerty and Armstrong, 1996). The same data set was used in the Brubaker et al (2000) study as described above. To focus the analysis on a region that is as homogeneous as possible over the footprint scale, a subset of these data have been selected . The subset represents an area west of the Ural Mountains (45-60 deg. N. Lat., 25-45 deg. E. Lon) where gauge station density is maximum (approximately one or more stations per 100 km). The terrain is non-complex (grassland steppe with maximum elevation differences of less than 500 m) and most of the region is non-forested.

The FSUHS data record extends to cover both the SMMR and the SSM/I periods allowing pre-launch analysis of both the low (6 and 10 GHz) and high frequency channels (85 GHz) which is comparable to the future AMSR-E. This gauge station data represents a unique and valuable source for algorithm validation. They include not only SWE values but additional information pertaining to snow structure including density and number and thickness of melt-freeze crusts, extent of snow cover within the surrounding terrain, as well as forest type and percent of forest cover from a 50 km diameter area surrounding the station. These transects are typically 1.0 to 2.0 km in length with measurements every 100 to 200 m and are representative of both open and forested locations. The linear transect data provide a unique opportunity to evaluate statistically the response of an algorithm to a spatial pattern that lies between a single point measurement typical of most reporting networks and the area integration represented by the satellite foot-print. These data have now been compiled and interpolated to the EASE-Grid format for use in this study. For each station file, the analysis involves the extraction from the NSIDC mass storage of daily brightness temperature files for the observation date and for the previous two days to provide complete spatial coverage. Algorithm output and station measurements are then compared over the complete period of available data using statistics which include average, maximum and minimum differences, root mean square (rms) differences and total number of pixels available for comparison.

3.3.3 Quality Control and Diagnostics

The first step in quality control will be visual examination of the snow water equivalent products to ensure that the SWEMAPs are consistent with our understanding of climate, and no gross errors are being made. We will further compare retrieved snow water equivalent values with snow water equivalent estimates from airborne gamma observations over the U.S. (Carroll, 1997). Due to very limited areal snow water equivalent data, we will also compare our estimates with snow gage data. We will utilize the kriging process (Carroll et al., 1993) to construct statistical relationships from the widely scattered snow gage measurements. We will continue comparing model generated areal snow water equivalent value of a basin and sub-basin with estimates derived from the algorithm. We will also compare SWEMAP with MODIS derived snow maps for comparison of snow extent. When a particular assumption is found to be deficient, we will employ a better procedure to correct the problem.

Diagnostic checks for out-of-range data or unreasonable results will be used in the algorithms to determine whether the output should be flagged as unacceptable. Some diagnostic checks may trigger alternative decision tests in the algorithm. An example of such diagnostics is determination of snow wetness. The snow retrieval algorithms are not expected to be reliable in wet snow conditions, but they may be used with appropriate adjustments as the melting season approaches. A diagnostic test may determine the amount of wetness in a scene, and based on that determination we can proceed with the snow decision tests or mark the data as ‘wet snow.’

3.3.4 Exception Handling

Most exceptions should be handled in the Level 1 processes. We will only address those items that are believed significant for Level 2 and Level 3 processes. Occasional missing-pixel data or missing lines of data may be worked around by flagging that missing data and proceeding with the algorithm, carrying that missing data flag through to the output data set. In cases where input data files are unavailable but necessary for completing intermediate calculations, the algorithm should not proceed until those data are available.

Numeric errors and out-of-range values are errors that may arise from equations in the algorithm. Numeric errors will be handled by flagging them, i.e., filling with a code value and continuing with processing the rest of the data set. Intermediate calculations will probably be checked for out-of-range values and filled with a code value if out-of-range values are detected.

If snow wetness is present for an entire 5-day period over a pixel or group of pixels, no usable snow water equivalent data could be generated and that will be indicated on the SWEMAP products. Pixels over permanent ice sheets will be flagged until the snow accumulation rate algorithm is completed.

Other predicted exceptions are as follows:

(a) Insufficient orbits at the Level 3 algorithm: If the minimum amount of data needed to compute credible pentad estimates is not met, the pentad product will be set to missing.

(b) Abnormal program termination: Unless the program termination code is set to normal termination, the appropriate error message will be sent to the operator. This will require immediate corrective action as needed.

(c) Files not found: The program will terminate and the appropriate error message will be sent to the operator.

(d) Fatal computation error: This will result in an abnormal termination.

(e) Non-fatal computation error: Warning messages will be sent to the operator who will decide whether to halt the processing or continue the processing until the problem can be resolved.

4.0 Constraints, Limitations, Assumptions

There are several known limitations that must be considered when using microwave observations to infer snow parameters. When the snowpack is wet, the measured

brightness temperature becomes similar to that of the bare ground. Therefore the microwave signature will not be able to determine successfully the amount of snow storage when the snowpack is wet. The data will be flagged as "wet snow." When it is raining, the data will be flagged as "rain" and no SWE estimated. In the mountainous regions when the average slope is larger than 0.3, this data will be flagged as "mountainous" and no SWE estimated. Post launch algorithm testing will review situations where adverse affects from rugged mountainous terrain can be reduced.

4.1 Error Analysis

Many error sources that could affect the snow water equivalent retrieval were mentioned in Sections 3.2.1, 3.2.2 and 3.2.3. We will try to quantify these errors individually. In addition, a significant source of error in mapping the snow storage is expected in situations of mixed pixels where snow signal is obscured or confused with vegetation cover, or in situations of patchy snow cover during transitional seasons. There are also errors in mapping snow in mountainous areas due to obscuration of snow by steep mountain slopes. Mis-registration of pixels in the EASE grid map projection may also contribute to an overestimation or underestimation of snow cover. Error estimates in these situations will come from validation studies, comparing SWEMAP-generated snow storage to other snow-cover data sets and/or ground observations.

4.2 Combination of AMSR-E and other EOS Data for Snow Mapping

Visible and infrared data have been used to map Northern Hemisphere snow cover since the mid 1970s. The limitations of using visible sensors include polar darkness and areas with persistent cloud and forest covers. During the high winter, solar incidence angle is low in the polar region. Solar reflectance from snow surface is also low which makes it difficult to detect snow cover. The combination of visible, near-IR, short-wave IR and microwave will lead to an improved ability to map snow extent, and water equivalent. Passive microwave sensors are generally unaffected by cloud and solar incidence angle. It will be advantageous, in the EOS era after the launch of the Aqua satellite, to use AMSR-E data in conjunction with MODIS data to map the snow extent. Microwave data will improve the snow mapping when cloud cover and low solar incidence angle limit the visible and infrared sensors. When the passive microwave sensors are unable to distinguish between wet snow and wet ground MODIS data will be used to assist in snow detection.

5.0 VALIDATION

Three types of approaches for snow validation will be designed. Type 1 is grid scale validation, based on comparing the SWE derived from aircraft measurements and satellite measurements. Type 2 is river basin scale validation, based on comparing SWE from snowmelt runoff model and satellite derived SWE, and Type 3 is regional scale validation, based on comparing the interpolated SWE values from point measurements with satellite derived SWE.

Type 1: Grid scale validation

The SWE products will be evaluated at the 25 km by 25 km EASE-Grid scale (Armstrong and Brodzik, 1995). This represents a scale that can be surveyed from aircraft with a reasonably high observation density. Sensors such as the airborne gamma SWE detector and multi-frequency microwave radiometers can provide over-flights of several EASE grid cells that will then be used to provide estimates of the grid scale SWE. Since these sensors require the aircraft to fly at a very low altitude, flat open areas will be selected for this purpose. In addition, aircraft derived SWE values will be compared with ground observations.

Type 2: River basin scale validation

In mountainous regions it is not always feasible to obtain SWE using a small aircraft. One method to evaluate the accuracy of areal SWE estimates in mountainous regions involves comparisons with water balance or stream flow outputs from a hydrological model. An example of such a model is the Snowmelt Runoff Model (SRM) which has been applied to many mountain catchments worldwide. (Martinec et al. 1983). The SRM can simulate successfully the runoff from snowmelt in a river basin. For mountainous terrain, we can use the snowmelt model to calculate the areal snow water equivalent that is needed for the basin to produce the observed runoff (Martinec et al. 1983). The Rio Grande basin above Del Norte in the State of Colorado has been selected for this purpose. The basin is about 3419 square km. Based on the amounts of snowmelt runoff recorded at Del Norte, the SRM has been deployed to infer the amount of snow storage in the basin. The model derived snow storage matches well with the contoured snow water equivalent. Data from 1979 to 1985 were used to derive the regression relationship between SRM snow water equivalent and microwave brightness temperature. When applying this to 1987 data, the predicted SWE was 39.4 cm while the actual value was 43.3 cm, a difference of 9 percent (Rango et al. 1989). Figure 3 shows the results of this study. River basins over different parts of the world with the size of several thousands square km will be selected for this effort.

With respect to the river basin scale approach, we will benefit from a new study at CU/NSIDC (NASA and NSF funded) that involves the development of an integrated

near-real time monitoring and historical analysis of the major components of the pan-Arctic hydrologic cycle. Output from the AMSR-E snow algorithm will be compared with river discharge data compiled by this project as well as with modeled values of distributed winter precipitation.

Type 3: Regional scale validation

There are a few regional scales SWE validation data sets beyond the FSUHS data sets described above. Unfortunately the FSUHS data are only available through 1990 at this time. In order to obtain surface station measurements of snow depth and water equivalent during the Northern Hemisphere winter of 2000-2001 and beyond to be used in the AMSR-E validation effort, CU/NSIDC is currently negotiating with the All-Russia Research Institute of Hydrometeorological Information, Obninsk, Russia, the Satellite Meteorology Institute, Beijing, China, the Cold and Arid Regions Environmental and Engineering Research Institute, Lanzhou, China and the Canadian IDS team CRYSYS.

We will also evaluate the potential of snow depth information collected by meteorological stations and SWE obtained by snow courses in the U.S. Carroll et al. (1995) reported using a kriging model to incorporate snow gage data to estimate areal SWE with some success. We will use a similar statistical method to provide optimum estimates of snow storage from the areas where sufficient measurements are available from the ground-based network. This statistical information will provide us an opportunity to objectively assess the quality of retrieved SWE for a large area.

5.1 Pre-Launch Validation Activities

5.1.1 Field Experiments and Studies

Snow grain size is one of the parameters affecting the emerging brightness temperature from snowpacks. Field experiments were organized during recent winters to study the snowpack density and grain size profiles. The first experiment took place in early February, 1997 in Wisconsin. This was a joint experiment with the MODIS snow and cloud groups as a part of the WINter Cloud Experiment (WINCE). NASA ER-2 aircraft equipped with the MODIS Airborne Simulator (MAS) and Millimeter-wave Imaging Radiometer (MIR) flew over test sites in Wisconsin and Minnesota. Results of this experiment has been reported by Tait et al. (1999b). Microwave data from the 90 to 220 GHz showed promising in snowpack characterization. Even under cloudy conditions, MIR data can be used to detect snow cover although it was more sensitive to the atmospheric conditions. Quantitative determination of the snowpack storage was not a straightforward task. *In-situ* 35 GHz handheld microwave radiometer data were also collected to study the microscopic interaction of snow grains with microwave radiation. SSM/I data from F-10 and F-13 satellites were also collected. Overall, however,

comparisons between the satellite observations and ground observations gave very positive results.

To study the relationship of snow crystal size and microwave brightness temperature, snow pit observations were taken over many sites around the Colorado River Basin. This was a joint NASA-USGS project to study the snow storage in the Rockies after the 1983 snowmelt runoff anomaly. We will continue to cooperate with USGS and USDA researchers in building up the database on snowpack and crystal size profiles. In the late February, 1997, a field site near Pinedale, Wyoming was selected. This is an area that gave consistently low brightness temperature observations from the SSM/I. To investigate further this anomaly, many snow pits were dug in this area. Snow crystal samples were taken and have been analyzed by an electron microscope. *In-situ* 35 GHz handheld microwave radiometer data were also taken to study the microscopic interaction of snow crystals with microwave radiation.

In developing the snow algorithm it has been found that the grain size distribution is the most critical parameter. With *a priori* snowpack grain size profiles built into the algorithm, snow retrieval accuracy can be improved. Recently, Josberger and Mognard (2000) developed an algorithm for snow depth that includes the effect of grain size growth that results from temperature gradient metamorphism [Colbeck (1987), Armstrong (1985)], and the general tendency of snow grains to increase in size with time. It is based on the cumulative effect of the temperature gradient through the snow pack as the winter progresses. The model uses a temperature gradient index (TGI), which is similar in concept to the cumulative heating or cooling degree-days. A linear relation was found between TGI and the spectral gradient, and this relationship can be solved for the snow depth as a function of time.

$$D(t) = \frac{-\alpha T_{air}}{\frac{d}{dt}(\Delta Tb)}$$

where D is the snow depth, t is time, T_{air} is the air temperature, and $\frac{d}{dt}(\Delta Tb)$ is the temporal rate of change of the spectral gradient. The algorithm assumes that the snow - ground boundary temperature is 0°C and it requires a time series data set for the air temperature. The snow depth depends on spectral gradient rate of change and not on its instantaneous value. Studies in the US northern Great Plains by Josberger and Mognard (2000) show that the strongest spectral gradient signatures emanate from regions with thinner snow packs. The new algorithm above captures this behavior while previous algorithms do not since they neglect temporal variations in grain size and assume them to remain spatially constant. However, thinner snow packs are subject to stronger temperature gradients and larger grains evolve more rapidly to yield a greater temporal change in the spectral gradient than would be the case for a thicker snowpack. This new

algorithm performs best when the daily values of air temperature and spectral gradient are smoothed over a two or three week period. The algorithm captures, therefore the monthly and seasonal behavior and eliminates daily fluctuations. We expect that it will work better for the Siberian case than for the snow in the U.S. Northern Great Plains because temperature gradient metamorphism is the dominant process controlling grain size growth in Siberia where temperatures are extremely cold. Because of the extreme cold we will investigate modifying the algorithm to use a non zero soil-snow interface temperature.

Field experiments will be conducted to collect snow grain size distributions and their variation with time. This is a part of the on going effort to create a comprehensive data base of snow crystal size profiles with different snow conditions. By collecting different snowpack profiles in different snow conditions for different events, we will be able to improve the model calculation of the brightness temperatures emerging from the snowpacks.

Field experiments over the Red River valley and Colorado River basin continued in the 1997-1998 winter season. These field activities are designed to improve our understanding of the evolution of snow grain size and spatial inhomogeneity of snow storage over a large area and to validate the pre-launch algorithm. SSM/I data have been used to test the pre-launch algorithm. Due to several logistical problems, 1999 snow field experiment was terminated early. For the winter of 2000 there was little snow accumulated in the snow sites, thus the experiment was cancelled.

A field campaign is planned for the 2000-2001 winter season. In conjunction with MODIS snow algorithm validation efforts, a field experiment will be conducted in New York state over the Adirondacks and Catskills. The emphasis is on obtaining spatially intensive samples of snowpack properties in an area where retrieval problems have been identified in the MODIS snow products. It is expected that a small, but expert team, will be able to collect a significant amount of data over a short period to coincide with SSM/I, MODIS, Landsat 7 and EO-1 overpasses. The ground data and optical data will be used for interpretation of microwave signals and further refine the AMSR-E snow algorithm described above.

A less comprehensive but still valuable snowpack data set is also to be collected in Keene, NH following on from the 1999-2000 winter campaign.

5.1.2 Comparison with Surface Observations

There are many snow gauges scattered around the world. Snow depth and snow water equivalent values vary greatly with time and space. When comparing the satellite estimates with ground observations, gauge measurements may not be representative of the entire microwave footprint. Over North America, National Operational Hydrologic

Remote Sensing Center (NOHRSC) routinely collects gamma data and gauge data over a large portion of the United States and part of Southern Canada. We are working with NOHRSC and USGS personnel to obtain these data and to produce areal averaged snow storage information. The first site to be selected is the Red River valley (which recently had a record snow and flood year) and data from 1989, 1994 and 1997 are now being analyzed.

Snow water equivalent and depth data are available from the limited snow courses scattered over the snow covered area. These sites are diminishing fast due to budgetary constraints and limited personnel available for these measurements. There are climatology and co-op stations in the US collecting snow depth data routinely and there are more than 600 automated USDA SnoTel sites in the mountainous regions of the western US providing daily SWE observations. Snow course and SnoTel data will be collected for comparison studies. The FSUHS snow course data described above are available for the years 1966 to 1990 from CU/NSIDC. Currently this data set is also being analyzed at GSFC. It is necessary to interpolate these point data before they can be used for comparisons with areal snow data. Substantial increases in funding would be required in order to speed up such comparison studies.

5.1.2.1 Lessons Learned from earlier studies (CU/NSIDC Project)

As noted above, the primary data set used in the initial phase of the CU/NSIDC SWE validation study is the "Former Soviet Union Hydrological Surveys" (FSUHS)(Haggerty & Armstrong,1996). At this stage we are simply evaluating the ability of the individual algorithms to reproduce the monthly climatology provided by the station data.

For each station file this involves the combination of the daily brightness temperature files for the observation date and for the previous two days to provide complete spatial coverage. SWE for all pixels containing at least one transect measurement are compared with the output from the respective algorithms. Results indicate a general tendency for the algorithms tested thus far to underestimate SWE. Underestimates of SWE increase significantly when the forest cover density exceeds 30 to 40 percent. Because of the detailed land cover data available for this validation study area, we will apply algorithm adjustments as a function of fractional forest cover using methods based on earlier work by Chang. et al. (1996).

5.1.3 Existing Satellite Data

Currently available multichannel satellite microwave data are from the DMSP SSM/I. SSM/I brightness temperatures are being used to emulate the AMSR data in developing the retrieval algorithm. For large area comparison between satellite estimates and ground observations, the FSUHS snow data will be used. We are cooperating with NSIDC researchers in this effort. Areal avaraged snow depth and snow water equivalent had been

compiled and compared with the satellite estimates. Time series of SSM/I data over selected sites for different snow classes (tundra, taiga, prairie, boreal forest and alpine) have been extracted for analysis. Due to sampling problems, we are still try to understand the temporal and spatial variation of snow storage when comparing the gage data and satellite derived SWE.

5.1.3.1 Lessons Learned from earlier studies (CU/NSIDC Project)

For the validation of snow extent, Armstrong and Brodzik (1998) compared microwave snow maps (SMMR and SSM/I) with the EASE-Grid version of the NOAA Northern Hemisphere weekly snow charts (Robinson et al. 1993). The original NOAA charts were derived from the manual interpretation of AVHRR (Advanced Very High-Resolution Radiometer), GOES (Geostationary Operational Environmental Satellite) and other visible satellite data.

The goal of this study is to determine if the differences between the algorithm output and the validation data are random or systematic. In the case of systematic differences, the patterns are being correlated with the specific effects of land cover type, atmospheric conditions and snow structure. Because we will compare algorithm output with continuous records of station data we will be able to identify any seasonal or inter-annual patterns in the accuracy of the algorithms.

For the 22-year study period the passive microwave and visible data show a consistent pattern of inter-annual variability and both indicate maximum extents consistently exceeding 40 million square kilometers (Figure 4). During this same period the trend in mean annual snow extent derived from both visible and microwave satellite data indicates a decrease of approximately 0.2 percent per year.

When the monthly climatologies produced by the two data sources are compared, results clearly show those time periods and geographic regions where the two techniques agree and where they tend to consistently disagree**.** During the early winter season (October through December) the passive microwave algorithms generally indicate less snow covered area than is indicated by the visible data (Figure 5). In both of these situations (shallow and/or wet snow) the microwave algorithms tested thus far are often unable to detect the presence of snow. However, preliminary results indicate that the inclusion of the 85 GHz channel, with the associated enhanced scattering response, improves the accuracy of mapping shallow snow, while algorithms which include the 37 GHz polarization difference improve the detection of wet snow.

5.2 Post-Launch Activities

5.2.1 Planned Field Activities

Type 1 experiment: Aircraft under-flight the AMSR overpasses

Based on the current Aqua satellite launch date, two aircraft missions are planned for February 2002 and March 2003. The 2002 snow flights will be coordinated and run jointly with the cold land mission. This is a major snow field experiment and will involve the NASA DC-8 (AIRSAR) and P-3 (PSR) aircrafts and the NOAA Chieftan aircraft (gamma sensors). For March 2003, the microwave sensors will be provided by the Technical University of Helsinki on the Skyvan aircraft.

(1) Colorado Experiment (February-March 2002)

Joint precipitation, snow and sea ice airborne experiments are planned for AMSR-E validation in January to March 2002. The snow validation campaign will be conducted jointly with EOS EX-7 core experiment (Cline, 2000) in February-March 2002. The joint experiment will have NASA DC-8 and NASA P-3 airborne laboratories over the Colorado and Wyoming. The Colorado and Wyoming sites represent the alpine and prairie snow types. Scanning microwave radiometer with AMSR-E frequencies and AIRSAR with C, L and P bands will be flown. Tentative flight lines over (Colorado sites) are selected. There will be over ten teams cordinated to measure the snow information on the ground.

During the sea ice experiment we will fly the Central Alaska and the Brooks Range of Alaska as a target of opportunity. The representative snow types in the Northern Alaska are tundra and taiga snow. Flight lines will be designed to cover several EASE grid on the ground for easy comparison with the AMSR-E SWE product. Extensive expert snow observations of snow parameters during the aircraft mission will be collected. .

Airborne gamma sensors have been used to monitor snow storage in the US for many years. Most of the data lines, of the order of 5 km each, are located in the mid-western part of US. We will cooperate with NOHRSC in this effort. Two test basins Rosael, MN and Black River, WI will be used for this part of validation effort. Gridded flight lines that cover an area 25 km by 25 km of the river basin will be flown in the 2002 winter. The gamma flights will be coordinated in the Colorado sites. Extensive ground measurements will be conducted during the aircraft flights. USGS, USDA and NASA researchers will participate in coordinating the flights and collecting snow data. These measurements will serve as the calibration points for the areal snow water equivalent values.

(2) Finland Experiment (March 2003)

This will be a joint effort with Technical University of Helsinki, University of Reading, USDA, USGS and NASA. Technical University of Helsinki will operate the aircraft and remote sensing instruments. Microwave radiometer consists of six frequencies (6.9, 10.7,

19, 23, 37 and 90 GHz). All other groups will contribute to the ground snow observations. Snow depth, density, grain size, underlying soil condition and forest cover distribution will be documented. Currently, two test sites are selected. They are Sodankyla, Finland at 67^{o}N, 26^{o}E and Kuusamo, Finland at 64^{o}N, 27^{o}E. Detail flight lines will be selected the summer of next year when we will be able to visit the sites in 2001. The flight lines will cover at least two 50 km by 50 km areas with different snow cover conditions.

Type 2: River basin scale validation

Six river basins located in north America, Europe and Asia are selected for this portion of the validation effort. They are (1) Rhine, Switzerland 3249 square km, (2) Rhone, Switzerland 3371 square km, (3) Rio Grande, Colorado, US 3419 square km, (4) Kings River, California, US 4000 square km, (5) Beas, Thalot, India 5144 square km and (6) Chatkal, Uzbekistan 6309 square km. Historical snow information, stream runoff data, temperature, precipitation, satellite microwave (SSM/I) data are being compiled. These ancillary data will be used to calibrate the snowmelt runoff model for the particular basin. Once the AMSR-E Level-2A data become available we will be ready to validate the satellite SWE estimates. We will conduct the river basin SWE validation for the next several winters.

Type 3: Regional scale validation

Regional scale studies depend on climate stations and co-op networks for snow depth and other weather information. Currently, the US is the only country with enough observations to allow us to pursue this effort. In the Northern Great Plains, the vicinity of the Red River basin of the North (43 – 49 ^{o} N;90 – 105^{o} W) will be the major site for validation. These data will be krigged to produce an areal snow map. Due to limited number of stations, the variance of interpolated snow maps will be large. MODIS and SSM/I derived snow products will be used as another sources of snow information for comparisons. We will try to extend the effort to Russia and Canada if we can routinely obtain the station snow data. The Ob River basin of Russia (60 – 80 ^{o} E; 48 –65 ^{o} N) and Canadian Prairie (49 – 53 ^{o} N; 90 – 110 ^{o} W) are the potential test areas.

5.2.2 Coordinated Field Campaigns

The Canadian EOS CRYSYS IDS team have planned a field campaign for the winter of 2002, probably during early February, in the Canadian prairies (agricultural land plus boreal forest) for the purpose of satellite microwave validation during the AMSR-E era. Depending on available funding, the plan will involve flights by a Twin Otter aircraft carrying the CRYSYS microwave radiometer (19, 37 and 85 GHz) plus newly acquired low frequency radiometers (1.4 and 6.9 GHz). It is the intention to coordinate these flights with flights of the NWS NOHRSC airborne gamma sensors. Other possible

locations for airborne campaigns include southern Ontario, central Quebec and the Mackenzie Basin.

5.2.3 Other Satellite Data

MODIS derived snow cover maps will be used to help determine the SWEMAP under more challenging snow conditions. Fractional snow cover within the AMSR footprint can be determined by aggregating the MODIS 500 m data. DMSP SSM/I or SSM/IS data with different overpass times will be used for comparison with the satellite estimates.

5.2.4 Other Data

In cooperation with NOHRSC and USGS personnel, airborne gamma data and gauge data over the North America will be collected and merged into areal snow information. NOHRSC routinely collects gamma data over the Northern US in spring. This information will be used for a comparison study over the snow season. Since validation effort requires time and resources, we will try to cooperate with other snow-covered countries in the validation effort.

The National Snow and Ice Data Center (NSIDC) has produced a 23 year time series of gridded satellite passive microwave data EASE-Grid format (Armstrong & Brodzik, 1999). This data set was developed using SMMR data for the period 1978 to 1987 and the SSM/I (Special Sensor Microwave Imager) data for 1987 to 2000. These EASE-Grid brightness temperatures provide the standard input to all algorithms being evaluated in this study.

5.2.5 Inter-comparison Study

Intercomparison studies are critical to consolidate the advancements in snow parameter estimates made by other researchers. The ideal time schedule for intercomparison activity is one year after the launch. This effort will involve assembling satellite and ground truth data sets for comparison. Additional man power and support funding are required to organize an international inter-comparison study to include additional snow investigators. We will collaborate with the Japanese AMSR team in this endeavor.

Algorithm inter-comparison projects will be organized to assess the quality of AMSR-E algorithm and algorithms developed by the Japanese AMSR scientists and other snow scientists. This activity will be conducted after we have collected several months of data over a snow season. Test areas located in different countries will be selected for this purpose. Results from these comparisons will help us to select the joint US/Japan standard snow products. With the imminent launch delay of the Japanese ADEOS-II satellite, this activity will be postponed to a later day.

We have also contacted B. Goodison of the Canadian IDS team CRYSYS on this matter. They showed interest in SWE validation in conjunction with their continued operational SWE program. We will include their SWE product in our comparisons.

6.0 References

Abdalati, W., 1996: Investigation of mass balance parameters on the Greenland Ice Sheet using passive microwave data. Ph.D. Thesis, University of Colorado, 131pp.

Armstrong, Richard L., 1985, Metamorphism in a subfreezing, seasonal snow cover: The role of thermal and vapor pressure conditions. Ph.D. thesis, Univ. of Colorado, 175 pp.

Armstrong, R.L., A.T.C. Chang, A. Rango and E.G. Josberger, 1993: Snow depth and grain size relationships with relevance for passive microwave studies. Annals of Glaciology 17, 171-176.

Armstrong, R.L. and Brodzik, M.J. 1995. An earth-gridded SSM/I data set for cryospheric studies and global change monitoring. Advances in Space Research, 16(10): 155-163.

Armstrong, R.L. & Brodzik, M.J. 1998. A comparison of Northern Hemisphere snow extent derived from passive microwave and visible remote sensing data. IGARSS-98, Proceedings: 1255-1257.

Armstrong, R.L. and M.J. Brodzik, 2000. Validation of passive microwave snow algorithms, IAHS Remote Sensing and Hydrology Symposium, Sante Fe, NM, April 3-7, 2000 (in press).

Barry, R.G. and A.J. Schweiger, 1988: Snow cover conditions in Northern and Central Europe. Final Report to NSF, SES-85/8586.

Basist, A., N.C. Grody, T.C. Peterson and C.N. Williams, 1997: Using the Special Sensor Microwave Imager to monitor land surface temperatures, wetness and snow cover. J. Appl. Metero. (in press).

Bromwich, D.H., R.-Y. Tzeng and T.R. Parish, 1994: Simulation of the modern arctic climate by the NCAR CCM1, Journal of Climate, 7, 1050-1069.

Brubaker, K.L., M. Jasinski, A. Chang and E. Josberger, 2000: Interpolating sparse surface measurements for calibration and validation of satellite derived snow water equivalent in Russia Siberia, Proceedings of the Remote Sensing and Hydrology 2000, Sante Fe, NM, April 2000.

Brun, E., P. David, M. Sudul and G. Brunot, 1992: A numerical model to simulate snow-cover stratigraphy for operational avalanche forecasting. J. Glaciology, 38, 13-22.

Carroll, T.R., 1997: Integrated ground-based, airborne, and satellite snow cover observations in the National Weather Service. 77th AMS Annual Meeting; Symposium on Integrated Observing Systems, Long Beach, CA.

Carroll, S.S., G.N. Day, N. Cressie and T.R. Carroll, 1995: Spatial modeling of snow water equivalent using airborne and ground based snow data. Enviornmetrics, 6, 127-139.

Chang, A. and L. Tsang, 1992: A neural network approach to inversion of snow water equivalent from passive microwave measurements. Nordic Hydrology, 23, 173-182.

Chang, A.T.C., J.L. Foster and D.K. Hall, 1987: Nimbus-7 derived global snow cover parameters, Annals of Glaciology, 9, 39-44.

Chang, A.T.C., J.L. Foster and A. Rango, 1991: Utilization of surface cover composition to improve the microwave determination of snow water equivalent in a mountainous basin. International Journal of Remote Sensing, 12, 2311-2319.

Chang, A.T.C., J.L. Foster and D.K. Hall, 1996: Effects of forest on the snow parameters derived from microwave measurements during the BOREAS winter field experiment. Hydrological Processes, 10, 1565-1574.

Chang, A.T.C., J.L. Foster, D.K. Hall, B.E. Goodison, A.E. Walker and J.R. Metcalfe, 1997: Snow parameters derived from microwave measurements during the BOREAS winter field experiment. JGR, 102, 29663-29671.

Chang, A.T.C., J.L. Foster, D. Hall, A. Rango and B. Hartline, 1982: Snow water equivalence determination by microwave radiometry. Cold Regions Science and Technology, 5, 259-267.

Colbeck, S.C., 1987, A review of the metamorphism and classification of seasonal snow cover crystals: IAHS Publication 162, p. 3-24.

Davis, P.A. and J.D. Tarpley, 1983: Estimation of shelter temperatures from operational satellite sounder data. Climate and Applied Meteorology, 22, 369-376.

Dewey, K.F. and R.Heim, Jr., 1981: Satellite observations of variations in Northern Hemisphere seasonal snow cover. NOAA Technical Report NESS 87.

Dewey, K.F. and R. Heim Jr., 1983: Satellite observations of variations in Southern Hemisphere seasonal snow cover. NOAA Technical Report NESDIS 1.

Ding, K.H., L.M. Zurk and L. Tsang, 1994: Pair distribution functions and attenuation rates for sticky particles in dense media. J. EM Waves and Applications, 8, 1585-1604.

Draine, B. and P. Flatau, 1994: Discrete dipole approximation for scattering calculations. J. Amer. Optical Soc., 11, 1491-1499.

Fily, M. and J.P. Benoist, 1991: Large-scale statistical study of Scanning Multichannel Microwave Radiometer (SMMR) data over the Antarctic. J. Glaciology, 37, 129-139.

Foster, J.L., A.T.C. Chang, D.K. Hall and A. Rango 1991: Derivation of snow water equivalent in boreal forests using microwave radiometry. Arctic, 44, Supp 1, 147-152.

Foster, J.L., D.K. Hall, A.T.C. Chang and A. Rango, 1984: An overview of passive microwave snow research and results, Reviews of Geophysics, 22, 195-208.

Foster, J.L., D.K. Hall, A.T.C. Chang, A. Rango, W. Wergin and E. Erbe, 1999: Effects of snow crystal shape on the scattering of passive microwave radiation. IEEE Trans. GRS, 37, 1165-1168.

Foster, J.L., 1995: Improving and evaluating remotely-sensed snow/microwave algorithms and snow output from general circulation models. Ph.D. thesis, The University of Reading.

Goodison, B., A.E. Walker and F.W. Thirkettle, 1990: Determination of snowcover on the Canadian prairies using passive microwave data. Proceedings of the International Symposium on Remote Sensing and Water Resources. Enschede, The Netherlands, 127-136.

Goodison, B.E., and A.E. Walker, 1993: Use of snow cover derived from satellite passive microwave data as an indicator of climate change. Annals of Glaciology, 17, 137-142.

Grody, N.C., 1991: Classification of snow cover and precipitation using the Special Sensor Microwave Imager. Journal of Geophysical Research, 96, 7423-7435.

Grody, N.C. and A.N. Basist, 1997: Interpretation of SSM/I measurements over Greenland. IEEE Trans. Geoscience and Remote Sensing, 35, 360-366.

Haggerty, C.D. & Armstrong, R.L. (1996) Snow Trends within the former Soviet Union. EOS, *Transactions American Geophysical Union*, Vol. 77, No. 46:F191

Hall, D.K., Foster, J.L. and A.T.C. Chang, 1982: Measurement and modeling of emission from forested snow fields in Michigan. Nordic Hydrology 13, 129-138.

Hallikainen, M.T., and P.A. Jolma, 1986: Retrieval of water equivalent of snow cover in Finland by satellite microwave radiometry. IEEE Trans. GRS, 24, 855-862.

Jordan, R., 1991: A one-dimensional temperature model for a snow cover. CRREL Special Report 91-16, 64pp.

Josberger, E.G., Mognard, N.M., (2000) A passive microwave snow depth algorithm with a proxy for snow metamorphism, to appear in, the Proceedings of the Fourth International Workshop on Applications of Remote Sensing in Hydrology. November 4-6, 1998, Santa Fe, NM. To appear in a special edition of the Journal of Hydrologic Processes.

Josberger, E., P. Gloersen, A. Chang and A. Rango, 1995: Snowpack grain size variations in the upper Colorado River basin for 1984-1992. JGR, 101, 6679-6688.

Kruopis, N., J. Koskinen, J. Praks, A.N. Arslan, H. Alasaalmi, and M. Hallikainen, 1998: Investigation of passive microwave signatures over snow-covered forest areas. IEEE IGARSS'98 digest.

Kunzi, K.F., S. Patil and H. Rott, 1982: Snow-cover parameters retrieved from Nimbus-7 Scanning Multichannel Microwave Radiometer (SMMR) data. IEEE Trans. GRS, 20, 452-467.

Marbouty, D., 1980: An experimental study of temperature-gradient metamorphism. Journal of Glaciology, 26, 303-312.

Martinec, J., A. Rango and E. Major, 1983: The Snowmelt-Runoff Model (SRM) User's Manual. NASA Ref. Publ. 1100, 11 8pp.

Matson, M., C.F. Ropelewski and M.S. Varnadore, 1986: An atlas of satellite-derived northern hemisphere snow cover frequency, National Weather Service, Washington, D.C., 75 pp.

Matson, M., 1991: NOAA satellite snow cover data, Palaeogeography and Paleoecology, 90, 213-218.

Matzler, C., 1987 Applications of the interaction of microwaves with the natural snow cover. Remote Sensing Rev., 2, 259-391.

Navarre, J.P., 1974: Modele undimensionnel d'evolution de la neige depose. La meteroroloie, 109-120.

Nolin, A. and J. Stroeve, 1996: The changing albedo of the Greenland Ice Sheet. Annals of Glaciology, (in press).

PLDS User's Guide, 1990: Nimbus-7 SMMR derived global snow cover and snow depth data set.

Pulliainen, J.T., J. Grandell and M.T. Hallikainen, 1997: Retrieval of surface temperature in boreal forest zone from SSM/I data. IEEE Trans. GRS, 35, 1188-1200.

Rango, A., J. Martinec, A. Chang, J. Foster and V. Van Katwijk, 1989: Average areal water equivalent of snow on a mountainous basin using microwave and visible data. IEEE Trans. on Geoscience and Remote Sensing, 27, 740-745.

Robinson, D.A. and G. Kukla, 1985, Maximum surface albedo of seasonally snow covered lands in the Northern Hemisphere. Journal of Climate and Applied Meteorology 24, 402-411.

Robinson, D.A., K.F. Dewey and R.R. Heim, 1993: Global snow cover monitoring: An update. Bulletin of American Meteorological Society, 74, 1689-1696.

Rott, H. and J. Aschbacher, 1989: On the use of satellite microwave radiometers for large scale hydrology, Proc. IASH 3rd Int. Assembly on Remote Sensing and Large Scale Global Processes, Baltimore, 21-30.

Snedecor, G.W., and W.G. Cochran, 1967: Statistical Methods, 6th ed., 593pp., Iowa University Press, Ames, Iowa.

Spencer, R.W., H. M. Goodman and R.E. Hood, 1989: Precipitation retrieval over land and ocean with the SSM/I: Identification and characteristics of the scattering signal. J. Atmo. Oceanic Tech., 6,254-273.

Sturm, M., J. Holmgren and G.E. Liston, 1995: A seasonal snow cover classification system for local to global applications. Journal of Climate, 8, 1261-1283.

Sun, C.Y, C.M.U. Neale and J.J. McDonnell, 1996: Snow wetness estimates of vegetated terrain from satellite passive microwave data. Hydrological Processes, 10, 1619-1628.

Tait, A. and R. Armstrong, 1996: Evaluation of SMMR satellite-derived snow depth using ground-based measurements. International J. Remote Sensing, 17, 657-665.

Tait, A., D.K. Hall, J.L. Foster and A.T.C. Chang, 1999a: High frequency passive microwave radiometry over a snow-covered surface in Alaska. Photogrammetric Engineering and Remote Sensing, 65, 689-695.

Tait, A., D. Hall, J. Foster, A. Chang and A. Klein, 1999b: Detection of snow cover using Millimeter-wave imaging Radiometer (MIR) data, Remote Sens. Environ, 68, 53-60.

Tsang, L., 1992: Dense media radiative transfer theory for dense discrete random media with particles of multiple sizes and permittivities. Progress in Electromagnetic Research, 6, 181-230.

Tsang, L. and J.A. Kong, 1992: Scattering of electromagnetic waves from a dense medium consisting of correlated Mie scatterers with size distributions and applications to dry snow. J. EM Waves and Applications, 6, 265-286.

Tsang, L. and J.A. Kong, 1980: Multiple scattering of electromagnetic waves by random distribution of discrete scatterers with coherent potential and quantum mechanical formalism. J. Appl. Phys., 51, 3465-3485.

Tsang, L., C.T. Chen, A.T.C. Chang, J.J. Guo and K.H. Ting, 2000: Dense media radiative transfer theory based on quasicrystalline approximation with applications to passive remote sensing of snow. Radio Science, 35(3), p.731.

Walker, A.E. B.E. Goodison, 1993: Discrimination of wet snow cover using passive microwave satellite data. Annals of Glaciology, 17, 307-311.

West, R.D., D.P. Winebrenner, L. Tsang and H. Rott, 1996: Microwave emission from density-stratified Antarctic firn at 6 cm wavelength. J. Glaciology, 42, 63-76.

Wiesmann, A. and C. Matzler, 1999: Documentation for MEMLS 98.1, Microwave emission model of layered snowpacks, IAP-Report 98-2, Inst. of Applied Physics, Univ. of Bern, Remote Sensing of Environment.

Williams, C.N., Basis, A., Peterson, T.C. and Grody, N. 2000 Calibration and verification of land surface temperature anomalies derived from the SSM/I, Bull. Am. Met. Soc., 81, 2141-2156.

Zurk, L.M., L. Tsang, K.H. Ding and D.P. Winebrenner, 1995: Monte Carlo simulations of the extinction rate of densely packed spheres with clustered and non-clustered geometrics. J. Optical Soc. Amer., 12.

Zwally, H.J., 1977: Microwave emissivity and accumulation rate of polar firn. J. Glaciology, 18, 195-215.

7.0 Table 1: Criteria for tests

(1) Surface temperature

Boreal forest (Pulliainen et al 1997)
T_{surf} (^{o}C) = 0.832 T_{19V} - 0.917 T_{19H} + 1.02 T_{22V} - 240.0

Alpine
T_{surf} (^{o}C) = -0.561 T_{19V} + 1.488 T_{22V} - 0.453 T_{37H} + 0.194 T_{85V} - 176.89

Taiga
T_{surf} (^{o}C) = 0.96 T_{19V} + 0.311 T_{22V} - 0.73 T_{37H} + 0.534 T_{85V} - 287.23

Prairie
T_{surf} (^{o}C) = -0.018 T_{19V} + 0.806 T_{22V} - 0.291 T_{37H} + 0.316 T_{85V} - 218.25

(2) Precipitation (Grody and Basist, 1996)

$T_{22V} > 258$ K
or
$T_{22V} > 254$ and SCAT < 2
or
$T_{22V} > 165 + 0.49\ T_{85V}$

where SCAT is the scattering index definded by Grody (1991).

(3) Wet snow

Snow wetness (% by volume, Sun et al, 1996)
$W_{snow} = -4.75 + 339.53\ T_D^{-1} - 6159.53\ T_D^{-2} + 40112.00\ T_D^{-3}$
where $T_D = T_{19V} - T_{37H}$

Wet snow/snow free discrimination (Walker and Goodison, 1993)
Wet $T_{37V} - T_{37H} > 10$ K, and $T_{surf} > 270$K

(4) Fractional forest cover correction

Ensemble of brightness temperatures for forested areas are calculated by linearly combining the forest free snowpack brightness temperature and the forest brightness temperature. Fractional forest cover is derived from the maximum albedo map (Robinson and Kukla, 1985).

$T_B = f\ T_{BF} + (1 - f)\ T_{BS}$

where T_B, T_{BF}, and T_{BS} are the brightness temperatures for mixed pixel, forest and snow, f is the fractional forest cover, and $T_{BF} = 0.9\ T_{surf}$. (Hall et al, 1982).

8.1 Schematic diagram of the MLP artificial neural network.

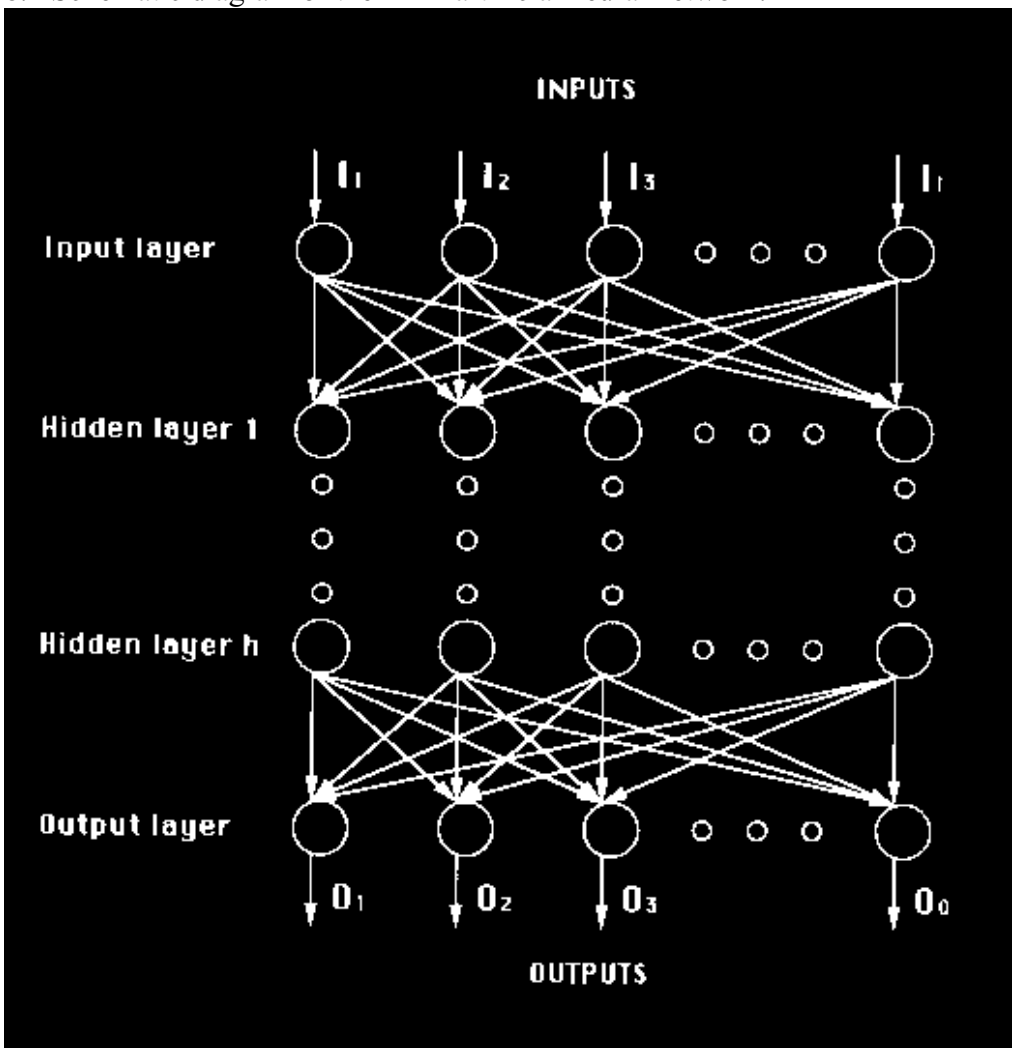

Figure 1

8.2 Schematic flow diagram of SWE algorithm

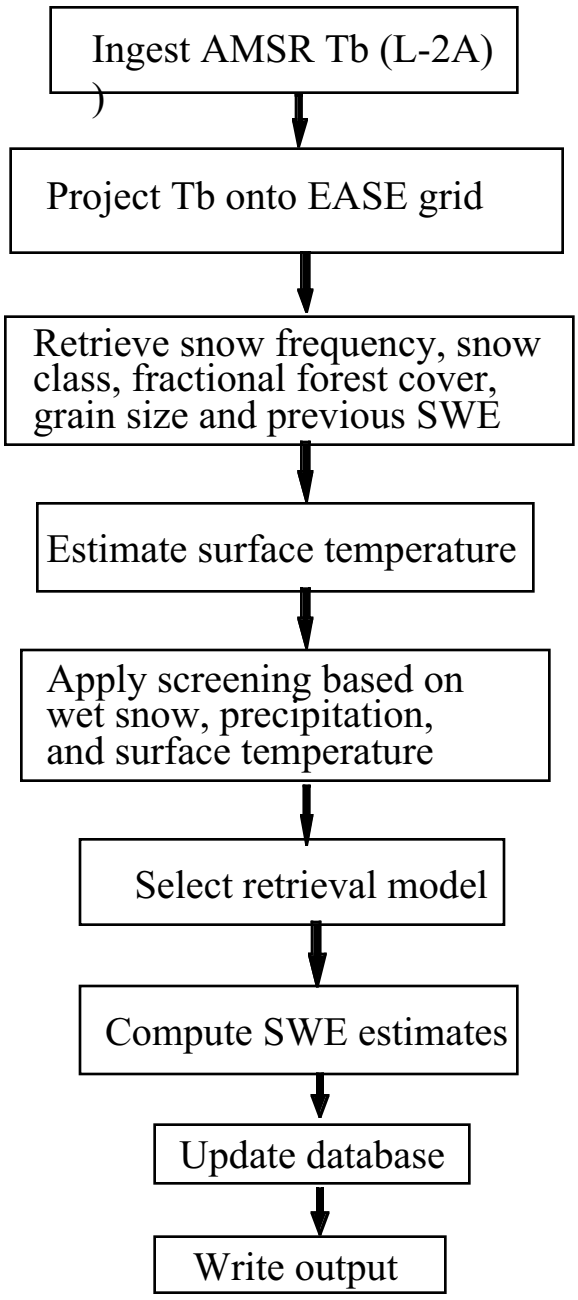

Figure 2

8.1 Comparison of SWE estimates from SMMR and SRM

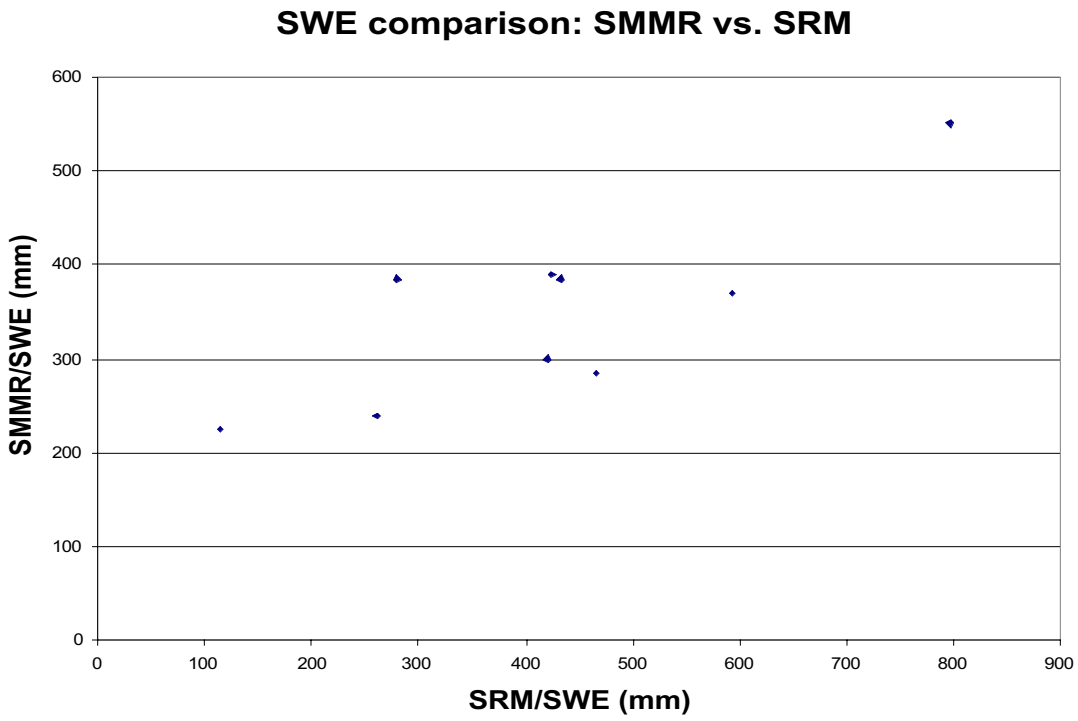

Figure 3

8.2 Northern Hemisphere snow-covered area (x 10^6 km^2) derived from visible (NOAA) and passive microwave (SMMR and SSM/I) satellite data, 1978-1999.

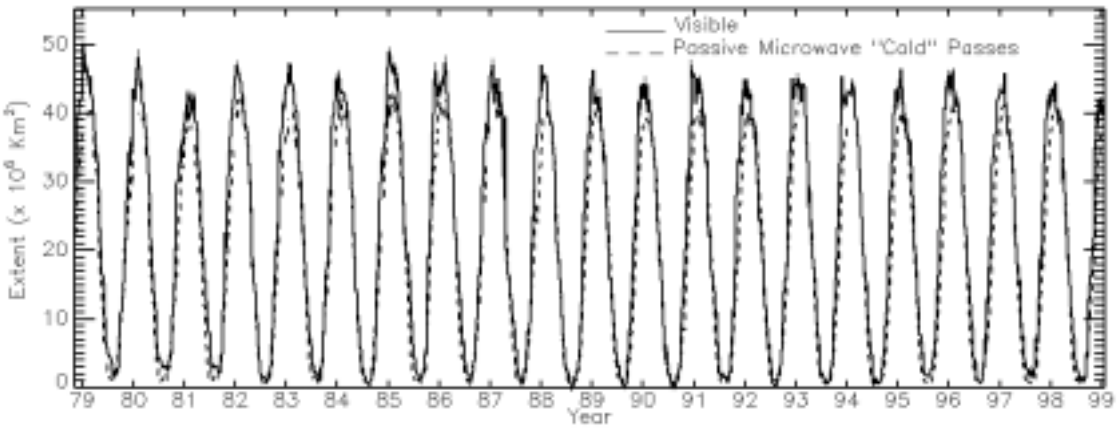

Figure 4

8.3 Average of total study area (FSUHS subset) snow water equivalent vs. passive microwave snow water equivalent using horizontally polarized difference algorithm, 1978-1990.

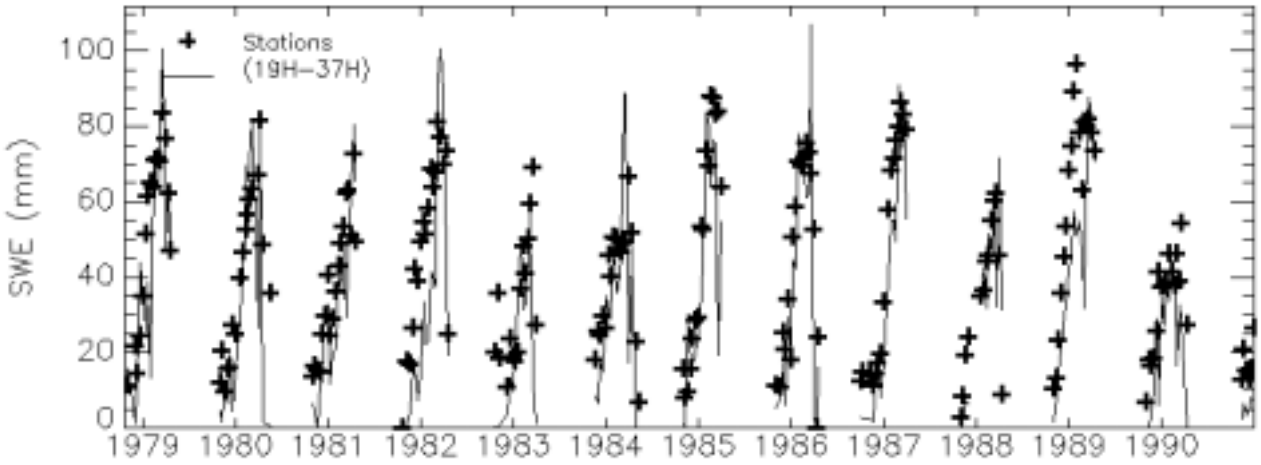

Figure 5